Original Research Paper

IJES *Iranian Journal of Earth Sciences*
Vol. 14, No. 1, 2022, 25-39.
DOI:10.30495/ijes.2021.1901981.1490

Origin and development of Skarn-Forming fluids from the Band-e-Narges Skarn Iron ore, Central Iran

Maliheh Nazari[1], Mohammad lotfi[*2], Nematollah Rashidnejad Omran[3], Nima Nezafati[4]

1. Department of Science College of Geology, Science and Research Branch, Islamic Azad University, Tehran, Iran
2. Department of Geology, Tehran North Branch, Islamic Azad University, Tehran, Iran
3. Department of Geology, Tarbiat Modares University, Tehran, Iran
4. Department of Geology, Science and Research Branch, Islamic Azad University, Tehran, Iran

Received 16 June 2020; accepted 19 January 2021

Abstract

The Band-e-Narges magnetite deposit is located in central part of Urumieh–Dokhtar Magmatic Arc (UDMA). Wide I-type calk-alkaline and alkalin magmatic activity in the Koh-e- Latif region has been reported due to Eocene intrusive processes in UDMA. The iron ores are hosted by Cretaceous limestone intruded by granite and granodiorite units. Genetic model of this deposit was determined using petrological, stable isotope, fluid inclusion and mineralographical data. Five stages of paragenesis were observed in terms of mineralization in this area: prograde stage, retrograde stage, sulfide-quartz stage, carbonate stage and oxidation stage. According to mineralogy and geochemistry studies, formation of the skarn has resulted from a hydrothermal fluid changing carbonate units to hydrosilicate minerals. The ore minerals showed magnetite features with slight chalcopyrite and pyrite. The $\delta^{34}S$ values ranged from +3.31 to +6.29 for the early retrograde stage pyrite and from +5.51 to +7.1 for that of late retrograde stage pyrite + anhydrite pairs. All the $\delta^{34}S$ values of pyrite and anhydrite + pyrite were positive with a magmatic sulfur origin in these deposits. Fluid inclusions were observed according to petrographic and microthermometric inclusions within garnet, quartz, and calcite minerals at various stages. Due to high temperature (414 -448 ºC) and middle salinity (up to 13.186 wt% NaCl) of fluid inclusions in prograde skarn-stage (garnet), the fluid inclusions showed a composition related to magmatic fluids following reaction with calcareous wall rock and fluid inclusions were trapped at pressures of 400 -500 bars, corresponding to depths of 1.5 -2 km in prograde stage. Fluid inclusions in quartz had moderate temperatures (152-303 ºC) and low salinity (7.9-11.3 wt% NaCl) indicating quartz-sulfide stage and late retrograde stage. The presence of fluid inclusions with moderate homogenization temperature (303 ºC) suggested that reboiling has occurred under hydrostatic pressure of 150-250 bars, equivalent to a depth of 1 -1.5 km in the late retrograde skarn and quartz-sulfide stages. Fluid inclusions in calcite had moderate temperatures (160 -287ºC) and low –to- high salinities (0.406-23wt% NaCl). A greater number of the fluid inclusions in the Band-e-Narges deposit had salinity (0.4-23.74 wt% NaCl) and homogenization temperatures (152-448 ºC) showing them as a moderate-high temperature and low–to-high salinity type of deposit. A decline in temperature and variation in salinity documented for the Band-e-Narges deposit would cause a notable decrease in Fe solubility and ore precipitation. Fluid compositions indicated that ore-forming fluid had a high fO_2 value and rich Fe concentration in the early stage, while having relatively lower fO_2 value and poor Fe concentration in the retrograde and sulfide stages. The data obtained from geology, mineralogy, geochemistry, salinities, and homogenization temperatures of the fluid inclusion populations at the Band-e-Narges iron deposit followed a model of boiling as a result of decrease in pressure, mixing, and cooling.

Keywords: *Iron Ore; Skarn; Geochemistry; Band-e-Narges; Fluid Inclusion; Sulfur Isotope*

1. Introduction

Urumieh-Dokhtar Magmatic Arc (UDMA) is a famous Iranian metallogenic belt and contains numerous major porphyry epithermal and skarn deposits related to Tertiary volcano-plutonic system and granite-related ore deposit. Iron skarn deposits are generally found in the UDMA including the Fe-Zn-W deposits in areas, such as Khot-PanahKuh, Hasht Kuh-khezr Abad, and Zero. The Band-e-Narges iron ore is situated in central part of northeastern margin of the UDMA about 205km NE of Isfahan City. It is ranked among the largest Iron skarn reserves in the region differing significantly from other iron skarns in terms of mineralogy and geochemistry. Ore resource of the deposit is equal to 0.2 Mt with 43% of Fe value.

---

*Corresponding author.
E-mail address (es):mo_lotfi@iau-tnb.ac.ir

Several studies have been carried out previously on mineralogy, petrography, geochemical, and geophysical characteristics of the deposit (Mohamadi 2006; Nazari 2015). Here, geological observation is applied together with mineral composition, textural and compositional data for magnetite, fluid inclusions, and composition of sulfur isotope to constrain origin for fluids and ore metals of the Band-e-Narges iron deposit and to provide new vision into genesis and evolution for sub-volcanic rock-hosted skarn deposit.

2. Regional Geology

The Zagros orogenic belt belongs to the collisional Alpine-Himalayan orogenic belt made by collision between the Arabian and Eurasian plates (Alavi 1994; Agard et al. 2005; Nazari 2015). The Zagros belt is divided into some tectonic units (Fig 1).

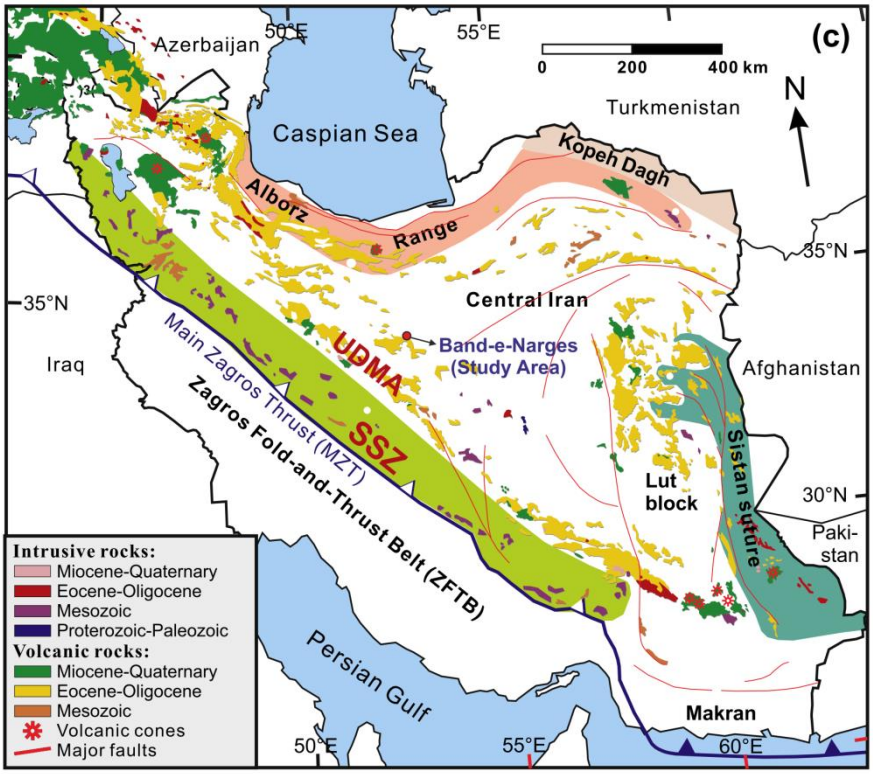

Fig 1. Simplified geological map of Iran showing the main tectonic subdivisions and locations discussed in the text (after Chiu et al. 2013).

It was made by three following geotectonic events (Alavi 2004); (A) subduction of the Neo-Tethyan oceanic plate beneath the Iranian litospheric microplates during Early to Late Cretaceous, (B) emplacement of several Neo-Tethyan oceanic silvers atop the African–Arabian passive continental margin in Late Cretaceous, and (C) collision of the African-Arabian continental Lithosphere with the Iranian microplates during and after Late Cretaceous. Late Triassic to Late Oligocene ophiolitic units close to the main Zagros reverse fault have shaped the suture between Arabia and Eurasia indicating Neo-Tethys oceanic lithosphere subducted beneath the Central Iranian continental plate (Nazari 2015). This collisional system represents its long-lived subduction–related magmatic activity since 150Ma along the UDMA with 50km of width (Ricou et al. 1977; Dercourt et al. 1986; Agard et al. 2005; Yazdi et al. 2019) spreading along the south Central Iranian microcontinent and supra-subduction zone (SSZ) (Fig 1). The main activity in the arc has happened between the initial Cretaceous subduction and peak of Eocene collisional magmatism (e.g., Stocklin 1974; Alavi 2007). Several intrusions have been made of different rocks, such as gabbro, granite, granodiorite, diorite bodies of various sizes (Haghipour 1977; Kananian et al. 2014; Sarem et al. 2021). Major Iranian Cu porphyry and Fe skarn deposits are associated with subduction and collision causing I-type magmatic activities in the UDMA (Atkinson and Eiaudi 1978; Einaudi 1982; Meinert 1992; Einaudi et al. 1981). Magmatic activity in the UDMA was started in the Eocene and continued until the Pliocene with its maximum intensity in the Middle Eocene (Mohajjel et al. 2000; Kananian et al. 2014; Mahdavi et al. 2015). The Band-e-Narges iron ore is located in central part of NE margin of the UDMA made by widely spread Late Eocene-Oligocene I-Type calc-alkaline and alkaline magmatic activity in this area (Mohamadi 2006; Nazari 2015) (Fig 2).

3. Geology of the Band-e-Narges Deposit

The Band-e-Narges iron ore deposit is a calcic skarn with assemblage of garnet (anderadite)-diopside-epidote-amphibole (tremolite), which can be divided into exoskarn and endoskarn zones. The Band-e-Narges skarn iron ore involves two main areas covering southern and northern zones. Formation of both well-developed endoskarn and exoskarn is the major characteristic of ore deposit (Fig 3).

Endoskarn is restricted to a narrow vein and to margins of the granodiorite, granite, and exoskarn. Mineral assemblage varies based on the distance from center of the deposits. The original igneous texture and mineralogy has been destroyed may be due to replacement of intrusive rocks by epidote and garnet-pyroxene along the contact with the exoskarn. The endoskarn consists of aluminosilicate minerals, quartz, pyrite, and calcite.

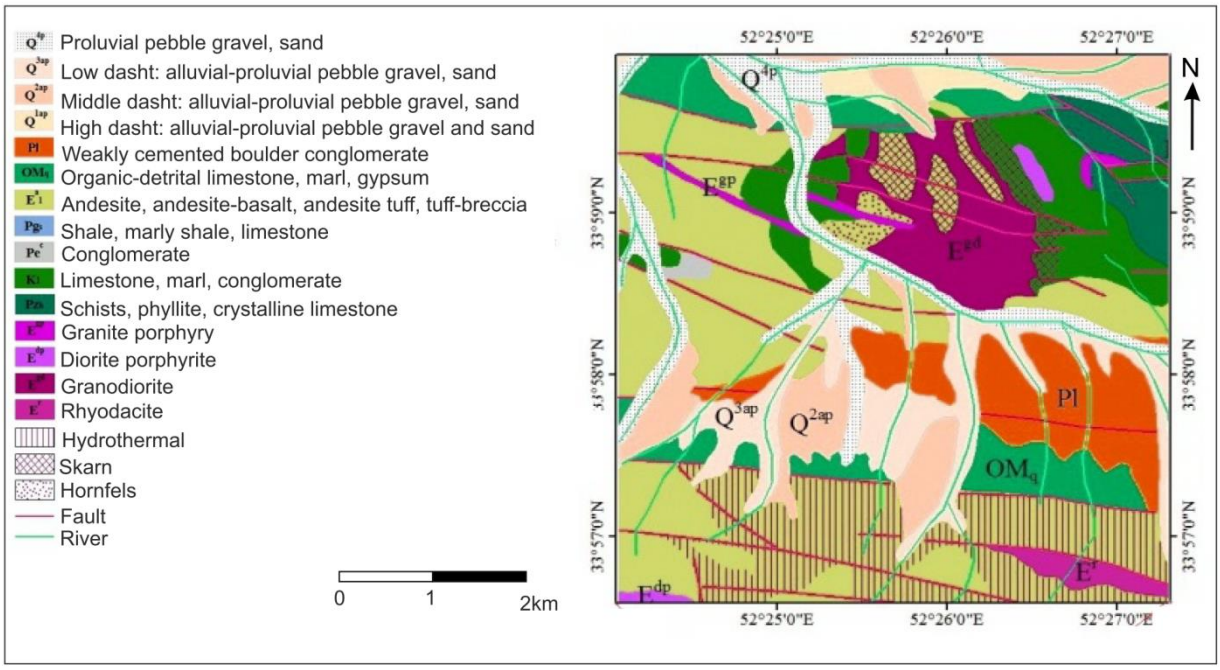

Fig 2. Geological map of the Band-e-Narges deposit and its location in the UDMA (adopted from Koh-e Latif 1:100.000 map, Geology Survey and Mineral Exploration of Iran).

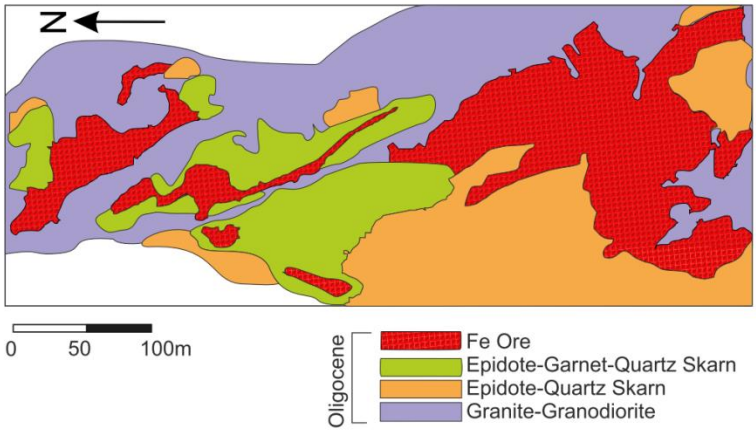

Fig 3.Geological map of the Band-e-Narges iron ore.

The exoskarn is divided into prograde and retrograde skarn assemblages enclosed by impure limestones and endoskarn, as depicted in Fig 4. These two areas do not differ significantly regarding skarn thickness and geometry because of features of the protoliths and intrusive rocks. Contact between the Cretaceous carbonate and intrusive rocks has led to variations in the protoliths and recrystallization to coarse-grained crystalline marble with an assemblage of garnet and pyroxene. Besides, skarn deposits are in close contact with intrusive body as well as crystalline limestone with similar mineral composition. Host rocks for skarn ores are Cretaceous impure limestones in northern and southern zones. The Eocene granites and granodiorites are situated in northern and eastern zones. The main structural features of the main faults include a NW-SE trend in the area and northern ore zones are mainly oriented in a NW-SE direction (Fig 3). In addition, alteration zones consist of iron oxidation and silicification with a minor propylitic alteration zone. Magnetite veins intergrown with calc-silicate minerals control the presence of limestones and carbonate-rich layers within the sequence. Two main iron ore mineralized zones have been introduced including magnetite zone and hematite zone. Magnetite is the major ore mineral extracted from this mine (Nazari 2015).

Mineralization

Exoskarn is divided into prograde and retrograde skarn assemblages (Fig 5) (Nazari 2015). This stage typically contains calcsilicates and massive iron oxide ore. A great bulk of the magnetite ore was formed during skarn alteration and replacement of limestone or volcanic host rock. Metasomatism of carbonate in the Band-e-Narges region has produced andradite-grossular, pyroxene and magnetite as components of the prograde assemblage and epidote, chlorite and quartz as components of the retrograde mineral assemblage (Nazari 2015).

Endoskarn: The epidote-quartz skarn zone has been well developed in southern zone (Fig 3). The endoskarn consists of quartz, chlorite, epidote, garnet, pyroxene, amphibole, pyrite, and calcite (Fig 5). Later, textual substitution of the early-formed calc-silicate minerals by oxides (magnetite, hematite) was observed in Fig 4 (a and d).

Sulphide-Quartz Stage: Sulfur and oxygen are ranked among the major volatiles significantly involved information of hydrothermal sulfide and oxide deposits (Mollai et al. 2014; Baratian et al. 2018). Pyrite is the most common sulfide in this deposit, along with chalcopyrite and covellite (Fig 4 e). Pyrites occur as cubes in massive veins (<3mm).

Carbonate Stage: The main skarn alteration is overprinted by a distinct phase characterized by massive zones of sulphide in center of deposits and calcite veins associated with potassic alteration.

Oxidation Stage: Goethite-rich oxidation zone covers both northern and southern zones (Fig 3). Martitization of magnetite is quite common mainly because of variations in oxygen fugacity (Fig 4 f and i).

Field and petrographical observations indicated the following stages of skarn occurrence:

(A) Prograde Stage: Pyroxene+ garnet +magnetite

(B) Retrograde Stage: Pyroxene+garnet+amphibole +epidote+chlorite+quartz+apatite

(C) Sulfide-Quartz Stage: Pyrite+ chalcopyrite+ covellite+ garnet+ chlorite+ quartz

(E) Carbonate Stage: Calcite +hematite+ goethite+ quartz

(D) Oxidation Stage: Hematite+ goethite+ quartz+ calcite

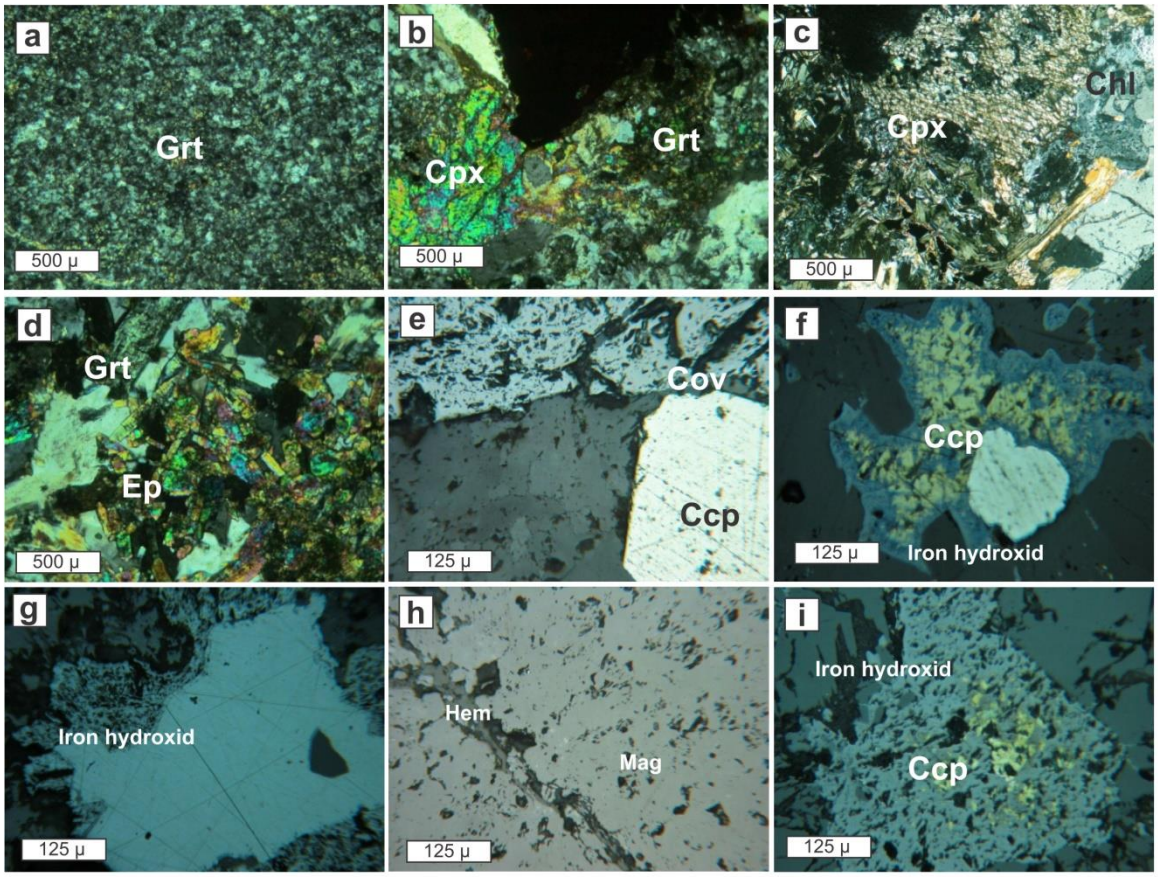

Fig 4. Microphotographs of thin sections for several rocks of the target area; a- Garnet in prograde stage; b- Coarse–grained changed clinopyroxene within isotropic garnet shows an earlier formation of the pyroxene; c- Interlayering of retrograde skarn with chlorite as well as change inpyroxene; d- Epidote after garnet and in retrograde skarn; e- A microphotograph of a polished section revealing replacement of chalcopyrite by covellite; f- Amicrophotograph of a polished section revealing oxidation zone (pyrite and chalcopyrite replacement by iron hydroxide); g- Microphotograph of a polished section displaying replacement of pyrite by iron hydroxide; h- A microphotograph of a polished section displaying replacement of radial magnetite by hematite because of martitization; i- Microphotograph of a polished section displaying replacement of pyrite by iron hydroxide.

The prograde stage is described by the created pyroxene, garnet, and magnetite (Fig 4). The retrograde stage is characterized by the presence of amphibole, epidote, and chlorite (Fig 4). During the prograde stage, significant amount of magnetite has been shaped. Quartz and calcite are the main gangue minerals in this stage and tend to vein into the early-formed minerals like garnet, clinopyroxene, and amphibole (Lingang et al. 2010). Skarn mineralization at the deposits similar to other iron-ore skarn deposits in the world was verified according to paragenetic study based on fieldwork and mineralographical study (Lingang et al. 2010). Prograde stage minerals like pyroxene, garnet, and magnetite are mainly anhydrous. The retrograde stage assemblage of minerals covers amphibole, epidote, and chlorite associated with oxidation. Development of various mineral assemblages was observed during sequential stages in Fig 5 including metamorphic, metasomatic and altered minerals in the form of hornfels, skarn and intrusive rock. A clear zonation was observed in skarn of the Band-e-Narges deposit and typical mineral assemblages in the skarns vary based on the distance from intrusive body.

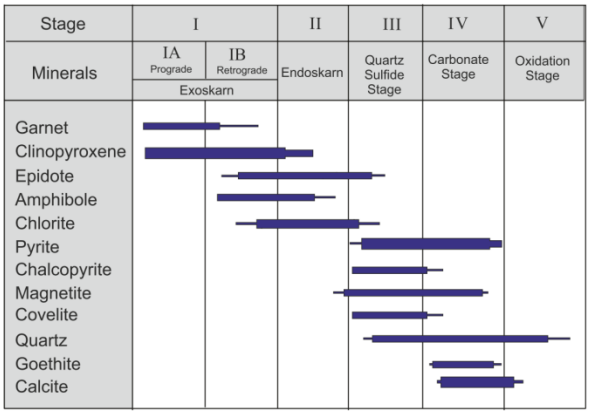

Fig 5. Schematic diagram showing paragenetic relationships of skarn and ore assemblages of the Band-e- Narges deposit. Widths of lines indicate relative abundances of minerals.

4. Sampling and Analytical Methods

In this study, 42 rock samples were used for petrographical and mineralographical studies as thin-polished sections. Compositions of minerals (Garnet_Pyroxene_Amphibole_Magnetite) were determined usingan electron probe microanalyzer (EPMA) at the Iranṡ mineral processing research center (IMPRC) for 15 rock samples. The selected samples from whole rock were analyzed in Australian SGS laboratories for major and trace elements. Furthermore, oxides were determined by X-ray fluorescence (XRF) in the Sarcheshme Laboratories. Fluid inclusion studies were conducted on more than 8 samples at the IMPRC on a LinkamTHMS600 stage with a temperature range between -196 -600ºC.A combination of heavy liquid techniques was used to concentrate pyrite mineral grains and then, handpicking was done. Visual estimation was done to determine purity of most of mineral concentrates with respect to other sulfur-bearing contaminations that was naturally greater than 99% according to optical examination by a binocular microscope. MAT251 gas isotope mass spectrometer was applied in the UK ISO Analytical laboratory for conducting isotopic analyses of SO_2.

5. Results

5.1. Mineral Chemistry

Garnet

EPMA data for garnet in the Band-e-Narges deposit are shown in Table 1 and Figs 6 (b and c) show a wide compositional range including: anderadite (45-69 mol.%, averaging 55mol.%) followed by grossularite (30-69 mol.%, averaging 48mol.%) and almandine- spessartine (9-18 mol.%). The Al-Fe difference could be because of local variations in temperature (Rose and Burt 1979). Formation of anisotropic garnet is due to fluctuations from Japan and Ayazmant Fe-Cu skarn from Turkey is richer in grossularite and Songun Cu skarn of Iran and garnet vein NE of Mazraeh Cu-Fe skarn deposit of Iran are richer in andradite compared to Band-e-Narges skarn deposit. Garnet vein of Mazraeh Cu-Fe skarn deposit NW of Iran and garnet vein of Band-e-Narges skarn approximately showed the same chemical behavior (Nazari 2015; Yazdi et al. 2016).

Magnetite

Results of EPMA for magnetite are presented in Table 2. Generally, TiO_2 content of magnetite was as follows: n=5 0-0.739wt% mean (Fig 7a and b). In the Ca+Al+Mn vs.Ti+Vdiagram, magnetite at Band-e-Narges deposit is plotted in ore close to the skarn field (Fig 7 b).

Pyroxene

Table 3 shows chemical composition of the pyroxene in the Band-e-Narges deposit as plotted in Fig 6a. Pyroxenes with diopside composition (from Di70 Hd30 to Di80 Hd20) in samples BN-10 were found locally in the contact zone (between the skarn and intrusive rock). They were substituted by magnetite, even though in some places, pyroxene and magnetite appeared to be cogenetic. The total Fe (expressed as FeO) content ranged from 4.4 to 6.93%. The MnO content was low, ranging from 0 to 0.23wt% (0.10wt.% on average). The Mn/Fe average ratio was equal to 0.019.

Amphibole

The results of microprobe analyses are given in Table 4. As shown in Table 4, amphiboles are rich in Fe and most of them belong to ferro-pargasite. Based on the amphibole nomenclature presented in the literature (Leake et al. 1997), Cl-rich amphiboles are mostly magnesio-hastingsite with minor pargasite (Fig 8).

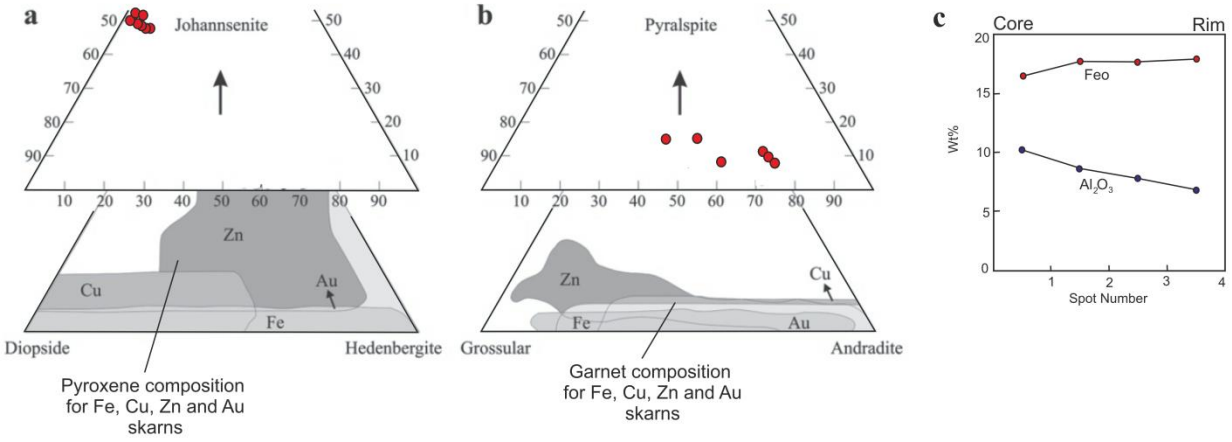

Fig6. (a) Ternary diagram displaying compositional difference in pyroxene from the Band-e-Narges deposit. (b) Ternary plot of garnet composition from the Band-e-Narges Fe ore and comparison of it with the same skarn. (C) Photomicrographs and composition of garnet in the Band-e-Narges iron ore showing the differences in FeO^T and Al_2O_3 of garnet grain along the profile.

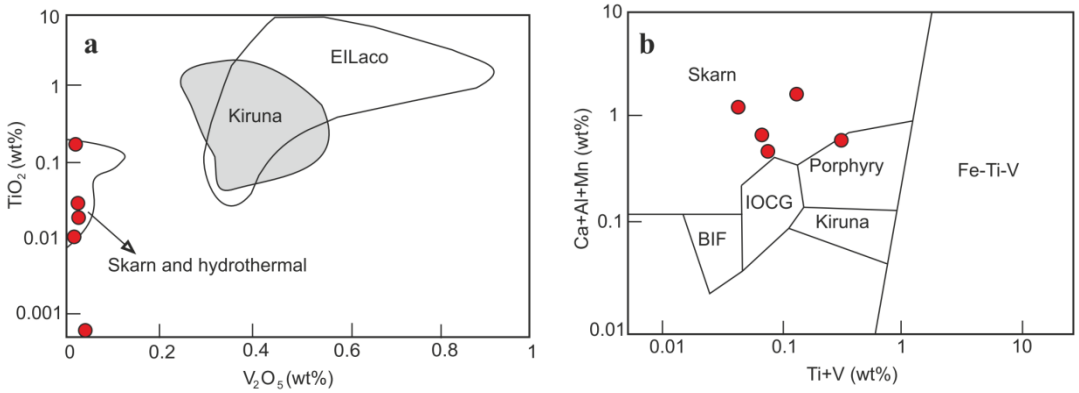

Fig 7. Compositional differences of magnetite from Band-e-Narges iron ore deposit and comparison of them with other skarn (a). Titanium +V vs.Calcium +Aluminum +Manganese diagram of magnetite from Band-e-Narges Fe ore (b). (Dupuis and Beaudoin 2011).

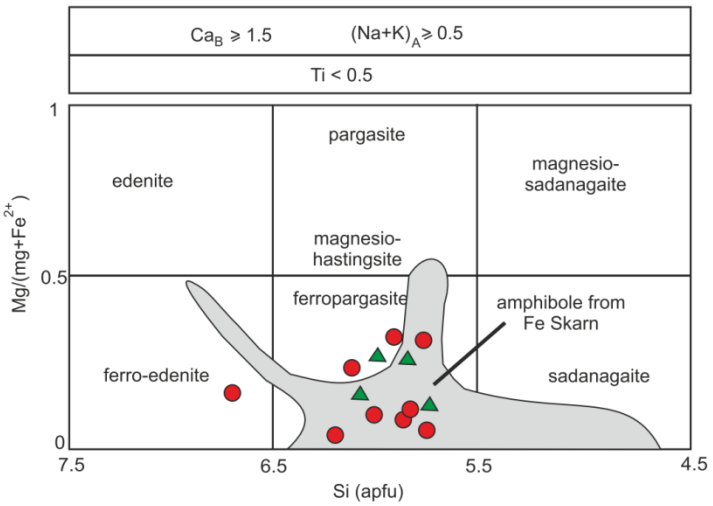

Fig 8. Comparison of amphibole from the Band-e-Narges skarn Fe deposit and amphibole from the Cihai deposit (Zheng et al. 2017) and other skarn Fe deposit (Pons et al. 2009).

Table 1. EPMA data of garnet obtained from the Band-e-Narges skarn deposit.

Sample	BN-13-1	BN-13-2	BN-13-3	BN-13-4	BN-13-5	BN-13-6	BN-9-1	BN-9-2	BN-9-3	BN-9-4	BN-19-1	BN-10-2	BN-10-3
SiO_2	38.1	37.68	37.64	40.39	40.2	40.12	41.95	41.16	39.52	38.63	40.48	39.26	42.16
Al_2O_3	6.06	5.9	5.86	27.23	25.45	27.14	10.16	8.73	7.79	6.93	24.88	25.1	24.75
FeO	22.03	21.92	21.73	9	11.31	9.19	16.59	17.85	17.81	18	8.68	10.92	7.12
MgO	0.13	0.11	0.1	0.01	0.05	0.04	0.37	0.29	0.14	0.14	0.07	0	0.16
MnQ	0.62	0.61	0.64	0.21	0.62	0.19	0.39	0.44	0.34	0.29	0	0	1.71
Na_2O	0.11	0	0	0	0.07	0	0	0	0	0	0	0	0.74
K_2O	0	0	0	0.01	0	0.01	0	0	0	0	0	0	0.02
TiO_2	0.66	0.75	0.64	0	0.03	0	0	0	0	0	0.13	0.07	0.02
CaO	33.18	31.8	31.93	23.79	23.08	24.17	32.54	32.32	33.67	32.40	23.76	23.43	21.85

Table 2. EPMA data of magnetite obtained from the Band-e-Narges skarn deposit.

Sample	BN-A-33	BN-A-34	BN-A-35	BN-A-36	BN-37
SiO_2	0.564	0.23	0.024	0.954	0.416
Al_2O_3	0.178	0.08	0.19	1.454	0.041
FeO	92.232	94.409	93.968	89.39	93.784
MgO					
MnQ	0.186	0.161	0.283	0.013	0.162
Na_2O					
K2O					
TiO_2	0.078	0.01	0.223	0	0.003
CaO					
V_2O_3	0	0.02	0.011	0.034	0.003

Table 3. EPMA data of pyroxene obtained from the Band-e-Narges skarn deposit.

Sample	BN-19-13	BN-19-14	BN-19-15	BN-10-1	BN-10-2	BN-10-3	BN-10-4	BN-10-5	BN-10-6
SiO_2	54.82	54.58	54.63	52.96	53.65	53.87	52.76	53.23	53.24
Al_2O_3	0.22	0.11	0	0.39	0.08	0.18	0.23	0.18	0.17
FeO	4.61	4.8	4.44	5.49	6.93	6.89	6.49	5.11	6.06
MgO	15.27	14.82	14.8	15	16.2	16.22	14.74	15.49	15.16
MnQ	0.18	0	0	0.23	0.04	0.04	0.3	0.02	0.16
Na_2O	0	0	0.44	0.42	0.2	0.13	0.24	0.18	0.18
K_2O	0.04	0.01	0.01	0.01	0	0	0.01	0	0.02
TiO_2	0.04	0.03	0.09	0.1	0	0.01	0	0	0
CaO	24.01	25.09	25.29	24.45	25.42	25.49	24.34	24.75	24.87
Total	97.19	97.44	99.7	99.05	99.52	99.83	99.11	98.96	99.86
Si	2.05	2.04	2.02	1.99	1.98	1.99	1.98	1.99	1.98
Al	0.00	0.00	.00	0.01	0.00	0.00	0.01	0.00	0.00
Ti	0.00	0.00	0.00	0.00	0.00	0.00	0.00	0.00	0.00
Fe^{+2}	0.08	0.09	0.14	0.17	0.12	0.12	0.20	0.16	0.19
Mn	0.01	0.00	0.00	0.01	0.00	0.00	0.01	0.00	0.01
Mg	0.85	0.83	0.81	0.84	0.89	0.89	0.83	0.86	0.84
Ca	09.96	1.00	1.00	0.98	0.01	1.01	0.98	0.99	0.99
Na	0.00	0.00	0.02	0.02	0.01	0.00	0.01	0.01	0.01
K	0.00	0.00	0.00	0.00	0.00	0.00	0.00	0.00	0.00
Ni	0.00	0.00	0.00	0.00	0.00	0.00	0.00	0.00	0.00

Table 4. EPMA data of amphibole obtained from the Band-e-Narges skarn deposit.

Sample	BN-A-1	BN-A-2	BN-A-3	BN-A-4	BN-A-5
SiO_2	38.85	39.91	39.18	39	38.81
Al_2O_3	10.98	9.33	9.93	9.28	9.44
FeO	29.34	27.62	31.95	32.77	32.15
MgO	3	3.71	1.17	1.05	1.30
MnQ	1.09	0.16	0.16	0.13	1.21
Na_2O	0.69	1.23	1.13	1.09	2.04
K_2O	2.79	1.50	2.24	2.35	0.18
TiO_2	0.00	0.11	0.19	0.03	0.14
CaO	11.71	11.11	10.51	10.40	10.43
F	0.33	-	0.28	0.33	0.31
Cl	2.91	1.40	2.16	2.72	2.21

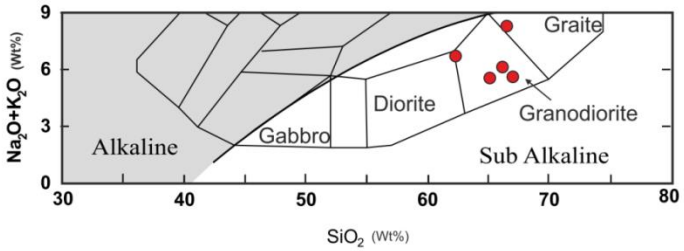

Fig 9. Plot of Na_2O+K_2O vs.SiO_2 for igneous rocks of Band-e- Narges deposit (Wilson 1989).

Table 5. Whole rock chemical composition of Band-e-Narges iron deposit.

Sample	SiO_2	Al_2O_3	FeOtot	CaO	Na_2O	K_2O	MgO	TiO_2	MnO	P_2O_5	SO_3	L.O.I	Be	Bi	Ce
BN-19	68.92	14.91	2.39	2.78	3.87	2.99	1.30	0.38	0.03	0.30		0.99	1.7	1.24	44.5
BN-1-2	64.50	15.94	5.12	4.09	4.26	2.80	2.23	0.69	0.07	0.47		1.70	1.4	1.08	19.5
BN-10-A	67.09	15.15	3.54	4.47	3.95	1.75	1.87	0.65	0.10	0.41		0.89	1.4	0.42	45.4
BN-2	66.56	15.60	4.89	3.65	3.85	2.98	2.13	0.66	0.06	0.44		1.22	1.5	0.51	46.1
BN-15	63.70	12.76	2.60	3.80	4.29	2.70	1.28	0.74	0.07	0.26		1.12	1.7	0.2	64.1

Samlpe	Co	Cs	Ga	Hf	La	Lu	Nb	Pb	Rb	Ta	Tb	Th	U	Y	Yb
BN-19	3.4	1.58	16.4	0.71	23.2	0.18	15.8	32	67.1	1.44	0.5	10.1	3	12.5	1.3
BN-1-2	12.1	1.1	14.2	1.13	7.2	0.15	18.5	23	11.8	1.71	0.29	4	0.4	10	0.9
BN-10-A	3.2	0.96	11.8	0.6	20.6	0.19	17.4	20	9.5	1.69	0.54	10.6	3.3	12	1.4
BN-2	5.2	0.56	15.2	1.23	22.4	0.23	21.8	136	10.2	2.01	0.65	7.5	0.9	17.1	1.7
BN-15	10.1	2.61	15.9	0.77	41.3	0.3	17.7	36	94.6	1.84	0.62	14.9	3.5	18	1.9

Samlpe	Ba	Ca	Cr	Cu	Fe	Mg	Na	Ni	S	Sr	V	Zn	Zr
BN-19	637	4.15	32	15.8	0.88	0.91	3.25	10.6	0.01	546	110	99	111.2
BN-1-2	136	1.85	43	13.6	3.3	0.4	4.98	8.2	2.7	549	90	50	132
BN-10-A	132	3.27	21	9.6	0.76	0.87	2.84	5.5	0.01	592	74	35	111.4
BN-2	121	3.1	97	35.2	1.61	1.23	5.35	8.3	0.01	673	134	251	128
BN-15	749	2.77	58	14.2	3.31	1.12	2.51	8.7	0.01	407	105	316	115.7

5.2. Geochemistry of Igneous Rock

Intrusive rocks exposed to the mining area were found to be dominated by Eocene granite and granodiorite having NS-trending structures (Fig 3). The results of whole rock analysis of igneous rocks in the region are reported in Table 5. As can be seen, they ranged from diorite to granite and granodiorite in terms of compositionin the SiO_2vs.Na_2O+K_2O diagram (Fig 9). According to the Rb vs. Y+Nb and Nb vs. Y (Fig 10) discrimination diagrams, igneous rocks were of I-type granite origin (Pearce 1996).

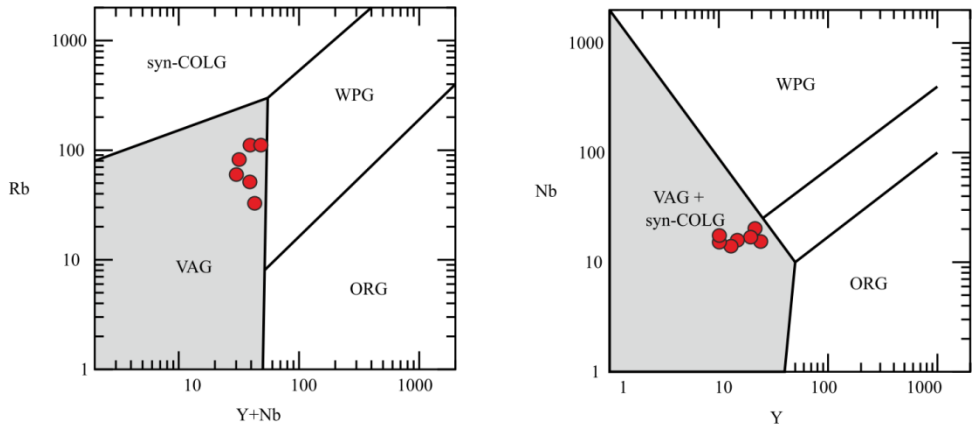

Fig 10.Variation diagram of Rb vs. Y+Nb and Y vs. Nb (Pearce 1996) displaying geotectonic environment of the magma.

Table 6. Sulfur isotope composition of pyrite and anhydrite from Band-e- Narges skarn Fe deposit.

Sample number	o^{34S} Values	Sample description
Early retrograde stage		
BN-32M	4.96	Pyrite+Magnetite
BN-2.3	3.99	Pyrite+Magnetite
BN-S2	3.31	Pyrite+Magnetite
BN-19W	6.29	Pyrite+Magnetite
Late retrograde stage		
SS1	7.1	Anhydrite+pyrite
SS2	5.51	Anhydrite+pyrite
SS3	6.2	Anhydrite+pyrite

5.3. Sulfur Isotope of Pyrite

A combination of heavy liquid techniques was done followed by handpicking to concentrate the pyrite mineral grains.

Table 6 shows the sample numbers, a brief description, and $\delta^{34}S$ values of pyrite and pyrite+ anhydrite. According to the analytical results, a narrow range of δ34S values (Fig 11) ranging from +3.31 to +6.29 (n=4, average of 4.63%) for the early retrograde stage pyrite and from +5.51% to +7.1(n=3, average of +6.27%) for that of late retrograde stage pyrite-anhydrite pairs was observed. According to the results obtained regarding all $\delta^{34}S$ values of pyrite and anhydrite+pyrite of the Band-e-Narges skarn Fe deposit, the values were significantly positive.

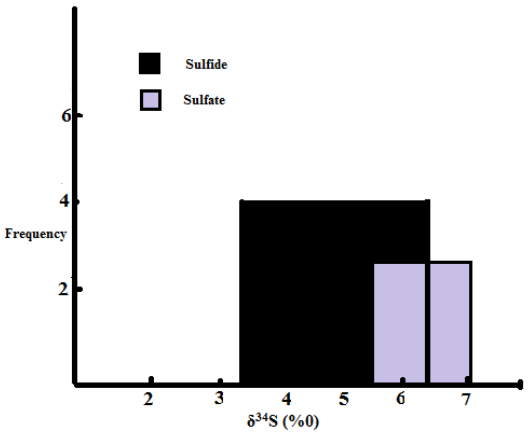

Fig 11. Sulfur isotopic compositions of sulfide and sulfate from the Band-e-Narges Fe deposit

5.4. Fluid Inclusion

Microthermometry was performed on fluid inclusions on a LinkamTHMS600 stage, with a temperature ranging between -196 -600ºC, mounted on a Zeiss microscope. Temperature of the stage was calibrated by heating: Cesium nitrate, at melting point of+414ºC and freezing: n-Hexane, at melting point of -94.3ºC. Precision of the measured temperatures was equal to±0.2ºC and ±0.6 ºC for heating and freezing, respectively. Salinity estimates were reported in weight percentage of NaCl equivalent calculated from the final melting temperatures of ice (Bodnar 1993).

Fluid inclusions in 8 samples under study with regard to garnet (prograde stage) and calcite minerals mentioned in the previous studies (Nazari 2015) and quartz found in the current study are shown in Table 7. The other 10 fluid inclusion sections remained unanalyzed since they were secondary or too small.

Fluid inclusions in the prograde garnet recognized at room temperature involved two phases, namely vapor-liquid inclusions (Fig 12a). All the studies on primary

double-phase fluids rich in vapor showed that they are made of vapor and liquid with a vapor volume of >70vol.% ranging from 5 to 7 µm in garnet size. Fluid inclusion sections were measured. Th values of (414-448°C) and (10.8-13.18wt.%NaCl equiv.) were obtained for temperature and salinity, respectively. Fluid inclusions trapped in quartz had Th values of 152-303°C and salinity of 7.9-11.3wt.%NaCl equiv. (Fig 12b). In calcite, two kinds of fluid inclusions were recognized at room temperature: (1) two phases: liquid-vapor type (2) three phases: liquid-vapor-halite type (Fig 12c and d).

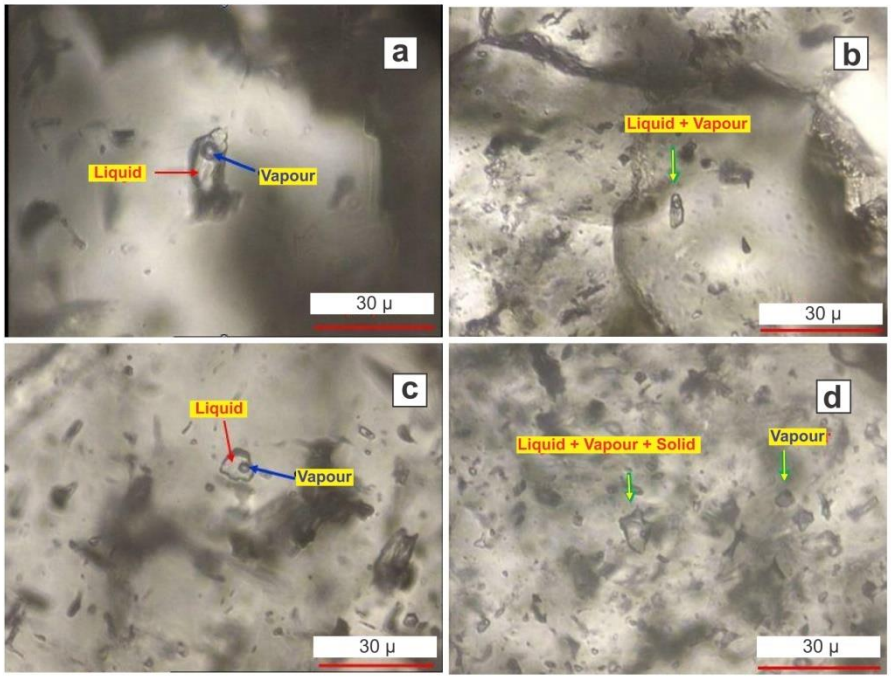

Fig 12. Fluid inclusions in skarn mineral from the Band-e- Narges iron deposit. (a)Vapor-rich fluid inclusions in garnet (prograde stage). (b) Comparatively large fluid inclusion section in quartz (sulfide-quartz stage). (c) Liquid- rich fluid inclusions in calcite. (d) Liquid-vapor-halite fluid inclusions in calcite

Table 7. Summary of microthermometric data obtained from fluid inclusions hosted in garnet, calcite, and quartz from the Band-e-Narges skarn deposit (Iran).

Sample	Host mineral	Fl type	Th(Range)	Mean	N	Tm(ice) Range	Mean	N	Salinity	Mean	N
BN-12	Gamet	Vapor+Liquid	414-448	431	10	-21.1 to -13.6	-17.35	7	10.8-13.18	11.99	7
BN-31	Quartz	Vapor+Liquid	152-231	191.3	5	-4 to -3.2	-3.6	3	7.9-9.11	8.50	
BN-32	Quartz	Vapor+Liquid	169-283	226	5	-5.3 to -3.8	-4.55	5	8.61-8.97	8.79	
BN-33	Quartz	Vapor+Liquid	250-303	176.5	4	-5.8 to -4.6	-5.2	3	8.18-11.3	9.74	
BN-23W	Calcite	Vapor+Liquid	168-203	182.5	4	-0.8 to -0.4	-0.6	4	0.406-1.18	0.75	4
BN-24W	Calcite	Vapor+Liquid+halite	169-203	186	5	-11.6 to -6.2	-8.9	4	14.469-14.75	14.60	4
BN-30B	Calcite	Vapor+Liquid+halite	160-287	223.5	14	-18.2 to -4.3	-11.25	10	7.53-23.746	15.63	10
BN-34	Calcite	Vapor+Liquid+halite	162-263	212.5	13	-11.3 to -2.3	-6.8	11	4.2-15.196	9.69	11

6. Discussion

Microthermometric results are shown in Table 7. Based on metasomatism, geochemical and fluid inclusion studies, 5 stages of mineralization were recorded in Band-e- Narges deposit.

Prograde Skarn Stage: Records for fluid inclusions included chemical compositions of the fluid inclusions and physicochemical conditions at the time of trapping. Samples with fluid inclusions are suitable for studying conditions of formation, migration, transformation, and evolution of hydrothermal fluids and finally, ore formation processes (Wilkinson et al. 2001). According to field observations and reports, formation of Band-e-Narges skarn deposit during several geological events

was similar to other skarn iron systems. Given high temperature (up to 448 °C) and medium salinity (up to 13.186% NaCl) of the fluid inclusions involved in garnet of the prograde stage in the Band-e-Narges deposit, magma composition has been formed after reaction with the wall rock (Kamvong et al. 2009). Reduction of pressure causes boiling and phase separation, leading to significant changes in temperature, pH, salinity, and oxidation state of ores (Drummond and Ohomoto 1985; Hedenquist et al. 1998). Boiling is caused by a sudden drop in pressure. This sudden drop in pressure is usually associated with fracturing or hydro-fracturing related to fluid pressures exceeding strength of overlying rocks (Roedder 1984). These stages have occurred during formation of Band-e-Narges skarn deposit, as there are fractures with NE-SW trend controlling distribution of ore.

The first boiling has occurred in the prograde stage as confirmed by the data for VL fluid inclusions at a temperature of 448 °C in garnet (Yellow zone) (Fig 13). According to the isothermal diagram of fluid inclusions (Hedenquist et al. 1998) trapping pressure of the fluid involved in the prograde phase was between 400-500 bars, corresponding to the lithostatic depth of 1.5 -2 km (Fig 13).

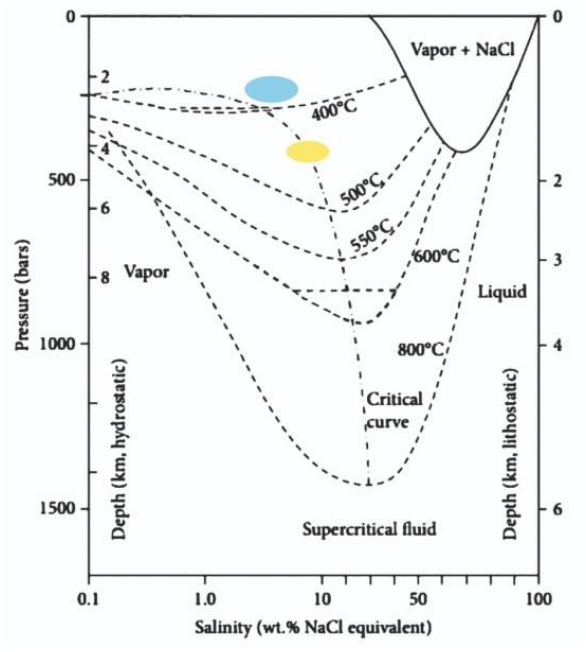

Fig 13. Isothermal P-T-X phase of fluid inclusions in the Band-e-Narges deposit (H_2O-NaCl system) (Hedenquist et al. 1998). Blue zone (first boiling), Yellow zone (second boiling). Schematic diagram of fluid inclusions shows the type of fluid inclusions generated at different salinities and same temperature and pressures during fluid phase separation.

Retrograde Skarn Stage: In addition, significant amounts of mineralization have been deposited in the Band-e-Narges iron ore deposit at temperatures up to 303 °C, a range that is lower in terms of Th values recorded in the fluid inclusions involved in the prograde stage. fO_2 value was decreased relative to the prograde skarn stage, which is in accordance with the existence of large amount of magnetite and hematite in the retrograde skarn stage (Zhang et al. 2018). Evolution of the Band-e-Narges ore rock-forming fluid included transfer of high amounts of $FeCl_2$ at high temperatures and high salinity (Mollai et al. 2014). The gases like H_2O and volatile H_2S, CO_2, and HCl have been continuously separated from homogeneous boiling liquid. In the next step, when the fluid had a temperature of 300°C, re-boiling has occurred, which caused excessive saturation and deposition of metal oxides and sulfides (Blue zone). Quartz sulfide phaseis characterized by fluid inclusions having medium temperature (153-303˚C) and low salinity (3.7-11.9 wt% of NaCl). Trapping pressure for the quartz-sulfide and late retrograde phases was about 150 -250 bars, as calculated by studying the depths of 1 -1.5 km under hydrostatic conditions, taking into account boiling of the liquid (Fig 13).

$3Fe^{2þ} þ 4H_2O \rightarrow Fe_3O_4$ magnetite $ÞÞ 6H^{þ} þ H_2$
$Fe^{2þ} þcu^{2þ} þ 2HS^{-} \rightarrow CuFeS_2$ chalcopyrite $ÞÞ 2H^{þ}$
$Fe^{2þ}þ 2HS^{-} \rightarrow FeS_2$, pyrite$Þþ 2H^{þ}$

Calcite Stage**:** The fluid inclusions involved in calcite showed a temperature of about 160 -287 °C with a salinity of 4.6 -23% NaCl. The minimum pressure at this stage was estimated to be 100 bars.Following emplacement of the intrusive rocks during the Eocene, hydrothermal fluids were discharged into a fractured rock around the magma. Veins for infiltration of fluid phases into early stage rocks could be made by these fractures. The prograde metasomatic stage possibly began at the onset of the magma formation. According to isotope studies, ore-forming materials of the Band-e- Narges deposit were originated chiefly from magma. It is likely that exsolution of volatile-rich phase from the magma has occurred accompanied with crystallization that together with metallic elements and chlorine has formed hot ore-bearing hydrothermal fluids with the sustained crystallization of the magma (Candela 1997; Hedenquist et al. 1998; Zhang et al. 2013). According to anhydrous silicates (andradite and diopside), metasomatizing fluids have transfered significant amount of the dissolved constituents into the skarn system. The fluids exsolved from developing magma could carry Fe,Si and Mg penetrating these elements into micro-fractures. Most Iron skarn deposits are found in the contact zone between an intrusive body with a strong oxidized environment and sedimentary beds having a strongly reduced environment (Einaudi et al. 1981; Zangh et al. 2013). The magmatic fluid has been probably directed from intrusions through marble, has migrated along permeable zone, and has

reacted with the host rocks to form prograde skarn assemblages. During the retrograde skarn stage, boiling and mixing of magmatic fluid with meteoric water input might have led to formation of epidote and other retrograde minerals (Einaudi et al. 1981). Reduced fluid temperatures were related to the increased efficiency of metal deposition (Zhou et al. 2017). These features may be due to boiling and mixing between magmatic fluids and external fluid sources and cooling. Mineral assemblages and fluid inclusion of the mineral clearly showed development of skarns in the Band-e-Narges area as they underwent changes from high-temperature to low-temperature conditions (Fig 14). The prograde stage specifically included contact metamorphism and prograde metasomatism, and the retrograde stage included early and late stages of retrogressive hydrous alteration.

The two evolutionary processes for the fluids that caused formation of the Band-e-Narges iron ore deposit are described as follows:

1. According to all the $\delta^{34}S$ values of pyrite and anhydrite+pyrite obtained from the Band-e-Narges skarn Fe deposit, the values were significantly positive (from 3.31 to 6.29%) and all anhydrites were meaningfully rich in $\delta^{34}S$ –related pyrite and the sulfides were formed from igneous rock fluid (Fig 15) (Hoefs 2009). After reduction in temperatures, Fe,Cu, and H_2S and other volatile phases exsolved from the magma and entered the low-temperature system developing sulfides and oxides. Based on significant amounts of calcite and hematite, pH and degree of oxidation in the skarn system changed during the late retrograde stage.

When the granodiorite is located at a depth of 1.5 -2 km, the magma has a temperature above 448 °C. This is considered as a closed system. A supercritical fluid accompanied by magma was located in upper part of the magmatic chamber. After ascending (from a depth of 1.5 -2 km) and a decrease inpressure, an immiscible fluid with temperature up to 448 °C and medium salinity up to 13.186% NaCl was created (boiling) as a result of progressive stage minerals (garnet and diopside).

2. Due to mixing with fluids, temperature was decreased and the fluid was created by moderate temperatures (152-303 ºC) and low salinity (3.5-5/8 wt% NaCl equiv.) (Fig 14).

Pressure was drastically reduced and secondary boiling caused formation of secondary minerals. In the skarn system, Cu, Al, and Ti were normally enriched in reducing environment and $Fe^{+3}$was enriched in oxidized environment (Ochiai et al. 1993; Nicolescu et al. 1998). In oxidant environments close to the intrusive mass, skarn ore deposits are easily formed with high proportions of garnet, pyroxene, and garnet with a combination of andradite rich in Fe^{+3}. Abundance of Fe^{+3}-rich epidote indicated that ore-bearing fluids related to the retrograde stage are still relatively oxidized. The permanent reaction between the mineral fluids and carbonates in the area was associated with a decrease in temperature and fugacity, which caused formation of a large amount of chlorite in the retrograde stage and sulfide-quartz stage.

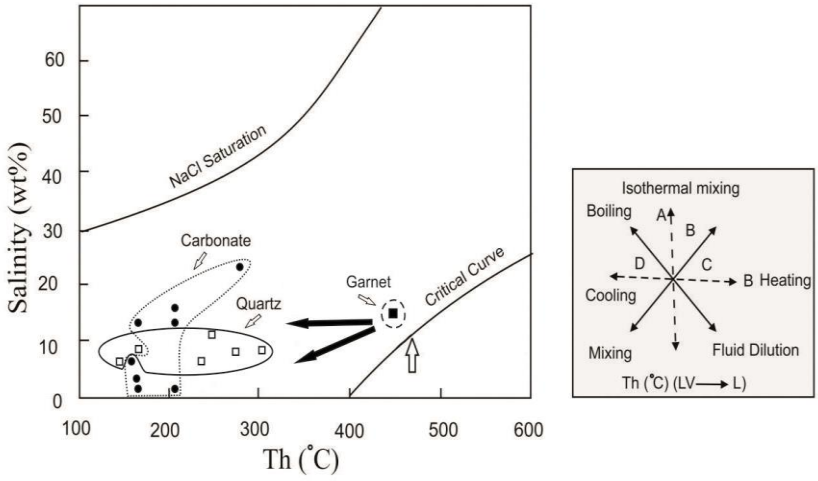

Fig 14. Plot of the measured salinities vs homogenization temperatures for skarn fluid inclusions from Band-e- Narges deposit. The right box shows temperature-salinity trends or fluid evolution paths caused by various geological processes (modified from Shepherd et al. 1985).

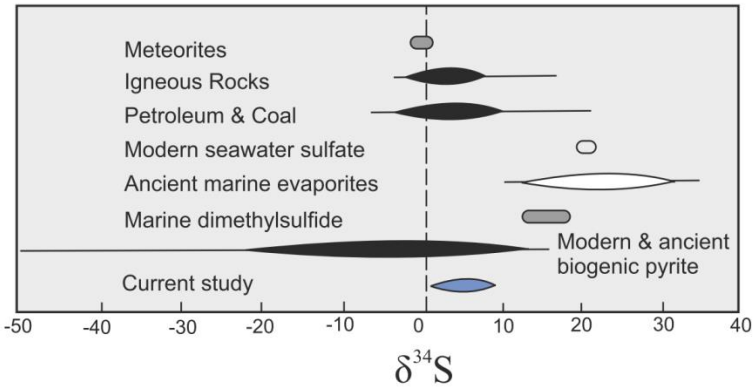

Fig 15. Pyrite $\delta^{34}S$ diagram of the Band-e-Narges deposit. Data were collected from the study by Hoefs (2009).

Interaction of Fe – bearing hydrothermal fluids with mafic minerals (such as biotite and hornblende) can lead to extraction of iron and magnesium and transfer of elements to other sites including fractures through metasomatism reactions, where these elements are precipitated in the form of other minerals. In other words, temperature decreases during crystallization and hydrothermal fluids rich in Fe, Si, and Mg are replaced by anhydrous silicates. Many hydrosilicates are formed, such as epidote, tremolite, as well as iron hydroxides. This area has well-developed fractures with NW-SE trend, which are good places for fluid passage and mineralization. Prograde and retrograde stages occur at high–to- moderate oxygen fugacity and a set containing andradite, magnetite, and hematite is formed. Continuous reduction of oxygen fugacity in the final retrograde stages and quartz-sulfide stage reduces sulfur from S^{+4}, S^{+6} to S^{-2} and creates suitable conditions for sulfide deposition (Hezarkhani et al. 1999).

7. Conclusions

The following conclusions were made according to findings of the present study:

1. Extensivelate Eocene-Oligocene I-Type calc-alkaline and alkaline magmatic activity in this regionhas led to formation of the Band-e-Narges iron ore deposit. Based on the geology, mineralogy, geochemistry and fluid inclusions data on this region, 5 stages of skarn occurrence were identified:

(A): Prograde Stage: Pyroxene+ garnet

(B): Retrograde Stage: Pyroxene+garnet+magnetite +amphibole +epidote+chlorite+quartz+apatite.

(C): Sulfide-Quartz Stage: Hematite+ Pyrite+ chalcopyrite+ covellite+ garnet+ chlorite+ quartz

(D): Carbonate Stage: Hematite+ goethite+ quartz+

(E): Calcite Oxidation Stage: Hematite+ goethite+ quartz

2. The prograde skarn stage indicated the presence of fluid inclusions with high temperature (414-448°C) and moderate-to-high salinity (10.8-13.18wt. %NaCl equiv.). Late retrograde and sulfide-quartz stage showed the existence of fluid inclusions with lower temperature (152-303°C) and salinity (7.9-11.3wt. %NaCl equiv.). Carbonate stage showed the fluid inclusions with lower temperature (160-287°C) and variable salinity (0.4-23.74wt. %NaCl equiv.). According to some reports, sulfur isotope can restrict origin of sulfur in the hydrothermal system ranging from 3.31 to 6.29% in the respective order, a magmatic sulfur origin was found in this deposit. Salinities and homogenization temperatures recorded from the fluid inclusion populations at the Band-e-Narges iron deposit followed a model of fluid mixing and cooling. A decrease in temperature and salinity documented for the Band-e-Narges deposit would cause a notable decrease in iron solubility and precipitation of massive magnetite.

3. Geology, mineral assemblages and composition, ore genesis and hydrothermal evolution processes of the Band-e- Narges skarn deposit were similar to many other calcic Fe skarns documented worldwide. Taken together, it can be concluded that the Band-e-Narges deposit is a typicalFe skarn deposit rather than it is associated with iron-rich melt as previously suggested.

The following fluid inclusions characteristics maybe used as exploration items in the Band-e-Narges deposit:

(A) The fluid inclusions had a middle temperature between 300-350 ºC.

(B) The fluid inclusions confirmed occurrence of the reduced pressures, boiling, cooling and fluid mixing.

References

Agard P, Omrani J, Jolivet L, Mouthereau F (2005) Convergence History Across Zagros(Iran):Constraints from Collisional fnd Earlier Deformation. *International Journal of Earth Sciences* 94: 401-419.

Alavi M (1994) Tectonic of the Zagros Orogenic Belt of Iran: New Data and Interpretation. *Tectonophysics* 38: 211-229.

Alavi M (2004) Regional Stratigraphy of the Zagros Fold-Thrust Belt of Iran and Its Proforeland Evolution.

American Journal of science 304: 1-20.

Alavi M. (2007). Structures of the Zagros Fold-Thrust Belt in Iran. *American Journal of science* 307: 1064-1095.

Atkinson JW, Einaudi MT (1978) Skarn Formation and Mineralizationin the Contact Aureole at Carr Fork, Bingham. *Economic Geology* 73: 1326-1365.

Baratian M, Arian MA, Yazdi A (2018) Petrology and petrogenesis of the SiahKuh intrusive Massive in the South of KhoshYeilagh, *Amazonia Investiga*, 7 (17), 616-629

Bodnar RJ (1993) Revised equation and table for determining the freezing point depression of H2O–NaCl solutions. *Geochimica Cosmochimica Acta* 57: 683–684.

Candela PA (1997) A Review of Shallow, Ore-Related Granites, Textures, Volatiles, and Ore Metals. *Journal of Petrology 38*: 1619-1633.

Dercourt J, Zonenshain LP, Ricou LE, Kazmin VG, Le Pichon X, Knipper AL, Grandjacquet C, Sbortshikov IM, Geyssant J, Lepvrier C, Pechersky DH (1986) Geological Evolution of the Tethys Belt From the Atlantic to the Pamirs Since The Lias. *Tethonophsics* 123: 241-315.

Drummond SE, Ohmoto H (1985) Chemical evolution and mineral deposition in boiling hydrothermal systems. *Economic Geology* 80(1):126-47.

Dupuis C, Beaudoin G (2011) Discriminant Diagram for Iron Oxide Trace Element Fingerprinting of Mineral Deposit Types. *Mineralium Deposita* 46(4)*: 319-335.*

Einaudi MT (1982) Description of Skarns Associated with Porphyry Copper Plution.Southwestern North America in: TitleySR (Ed), Advances in Geology of the Porphyry Copper Deposit, Southwestern North America. *The University of Arizona Press, Tucson*, 139-184.

Einaudi MT, Meinert LD, Newberry RJ (1981) Skarn deposits. *Economic Geology* 75: 317-391.

Haghipour A (1977) Geological Map of the Biabanak – Bafg Area 1:500,000.

Hedenquist HW, Arribas JR, Reynolds TJ (1998) Evolution of An Intrusion-Centred Hydrothermal System:far Southeast-Lepantoporphyry and Epitermal Cu-Au Deposits,Philippines. *Economic Geology*93: 373-404.

Hezarkhani A, Williams- Jones AE, Gammons CH, (1999) Factor controlling copper solubility and chalcopyrite deposition in the sungun porphyry copper deposit, Iran.*Mineral Deposita* 34: 770-783.

Hoefs J (2009) Stable Isotope Geochemistry, Sixth ed.SpringerVerlag, *Berlin*: 1-285.

Kamvong T, Zaw Z (2009) The Origin and Evolution of Skarn -Forming Fluids from the Phu Lon Deposit, Northern Loei Fold Belt, Thailand: Evidence from Fluid Inclusion and Sulfur Isotope Studies. *Journal of Asian Erath Sciences* 34: 624-633.

Kananian A, Sarjoughian F (2014) Geochemical Characteristics of the Kuh-E Dom Intrusion, Urmieh-Dokhtar Magmatic Arc (Iran): Implications for Source Regions and Magmatic Evolution. *Journal of Asian Earth Sciences 90*: 137-148.

Leake BE, Woolley AR, Arps CE, Birch WD, Gilbert MC, Grice JD, Hawthorne FC, Kato A, Kisch HJ, Krivovichev VG, Linthout K (1997) Nomenclature of amphiboles; report of the Subcommittee on Amphiboles of the International Mineralogical Association Commission on new minerals and mineral names. *Mineralogical Magazine* 61(405):295-310.

Lingang X, Jingwen M, Fuguan Y, Hennig D, Jianmin Z (2010) Geology,Geochemistry and Age Constraints on the Mengku Skarn Iron Deposit in Xinjiang Altai, Nw China. *Journal of Asian Earth Sciences* 39: 423-440.

Mahdavi M, Dabiri R, Hosseini ES (2015) Magmatic evolution and compositional characteristics of tertiary volcanic rocks associated with the Venarch manganese mineralization, SW Qom, central Iran. *Earth Sciences Research Journal* 19(2):141-5.

Meinert LD (1992) Skarn and Skarndeposits. *Geoscience Canada Reprint Series* 6: 117-134.

Mohajjel M, Fergusson CL (2000) Dextraltranspression in Late Cretaceous Continental Collision Sanandaj-Sirjan Zone Western Iran. *Journalof Structural Geology* 22: 1125-1139.

Mohamadi P (2006) *Mineralogy, Geochemistry of Band-E Nrges Iron Deposit, Southeastkashan. Published M.Se. Thesis.* (M.Se), ShahidBeheshti University.

Mollai H, Pe-Piper G, Dabiri R (2014) Genetic Relationship between Skarn Ore Deposits and Magmatic Activity in the Aharregion, Western Alborz, NW Iran. *GeologicaCarpathica 65*: 207-225.

Nazari M (2015) *Mineralogy, Geochemistry and Genesis of Band-E Narges Iron Deposit, Southeast Kashan.* (PhD), Islamic Azad University, Science and Research Branch, Tehran, Iran.

Nicolescu S, Cornell DH, Sodervall U, Odelius H (1998). Secondary Ion Mass Spectrometry Analysis of Rare Earth Elements in Grandite Garnet and Other Skarn Related Silicates. *European Journal of Mineralogy*10: 251-259.

Ochiai K, Tagiri M, Tanaka H (1993) Behavior of the Rare Earth Elements during the Skarn Formation at the Kamaishi Mine, Japan.*Resource Geology*43: 291-300.

Pearce J. (1996) Sources and settings of granitic rocks. *Episodes1* (19):120-5.

Pons JM, Faranhini M, Meinert L, Recio C, Etcheverry R (2009) Iron Skarns of the Vegas Peladas District, Mendoza, Argentina. *Economic Geology*104: 157-184.

Ricou LE, Braud J, Brunn JH (1977) Le Zagros, in Livre A La Memorie De A.F.De Lapparent(1905-1975).Memoire Hors Serie De La Societegeologique De France 8: 33-52.

Roedder E (1984) Fluid Inclusions. *Reviews in Mineralogy* 12: 644 p.

Rose W, Burt DM (1979) *Hydrotermal alteration, pp.173-235, in H.L Barnes, ed., Geochemistry of hydrothermal ore deposit, 2nd ed., Hohn Wiley & Sons,*

New York,798p. : Hohn Wiley & Sons, New York.

Sarem MN, Abedini MV, Dabiri R, Ansari MR (2021) Geochemistry and petrogenesis of basic Paleogene volcanic rocks in Alamut region, Alborz Mountain, north of Iran. *Earth Sciences Research Journal* 25(2):237-45.

Shepherd TJ, Rankin AH, Alderton DHM (1985) *A Partical Guide to Fluid Inclusion Studies*: Glasgow: Blackie; New York: Distributed in the USA by Chapman and Hall.

Stoklin J (1974) *Stratigraphic Lexicon of Iran: Part1*: Geological Survey of Iran.

Wilkinson JJ (2001) Fluid Inclusions in Hydrothermal ore Diposits. *Lithos 55*: 229-272.

Yazdi A, Ashja-Ardalan A, Emami MH, Dabiri R, Foudazi M (2019) Magmatic interactions as recorded in plagioclase phenocrysts of quaternary volcanics in SE Bam (SE Iran), *Iranian Journal of Earth Sciences* 11(3): 215-224.

Yazdi A, ShahHoseini E, Razavi R (2016) AMS, A method for determining magma flow in Dykes (Case study: Andesite Dyke). *Research Journal of Applied Sciences* 11(3): 62-67.

Zhang L, Jiang ShY, Xiong SF Duan DF(2018) Fluid Evolution of Fuzishan Skarn Cu-Mo Deposit from the Edong Disterict in the Middle-Lower Yangtze River Metallogenic Belt of China: Evidence from Petrography, Minerall Assemblages, and Fluid Inclusions.*Hindawi Geofluids*, 25 Pages.

Zhang Z, Du Y, Zhang J (2013) Alteration, Mineralization, and Genesis of the Zoned Tongshan Skarn-Type Copper Deposit, Anhui, China. *Ore Geology Reviews* 53: 489-503.

Zheng J, Mao JW, Yang F, Chai F, Zhu Y (2017) Mineralogy,Fluidinclusions and Isotopes of the Cihai Iron Deposit,Easterntianshan,Nwchina:Implication for Hydrothermal Evolution and Genesis of Subvolcanic Rock-Hosted Skarn-Type Deposits. *Ore Geology Reviews* 86: 404-425.

Zhou Z, Mao J, Che H, Ouyang H, Ma X (2017) Metallogeny of the Handagai skarn Fe–Cu deposit, northern Great Xing'an Range, NE China: Constraints on fluid inclusions and skarn genesis. *Ore Geology Reviews:* 80:623-44.